Performance analysis of IEEE 802.11e enhanced distributed channel access (EDCA)

Pradyot Kanti Hazra, Associate Professor [1], Asok De, Professor [2]

[1]Department of Computer Science, University of Delhi, Delhi - 110007, India.

[2] Department of Electronics & Communication Engineering, Delhi Technological University, Delhi, India.

Corresponding Author Email: pkhazra@cs.du.ac.in

Abstract

In this research article, we have proposed an analytical model for the   performance analysis of the enhanced distributed channel access (EDCA) protocol of IEEE 802.11e wireless local area networks standard, using four-dimensional Markov chain. The contemporary EDCA models support only a small subset of EDCA features with limited accuracy. Our model accurately covers all salient features of standard EDCA, like multiple numbers of simultaneously active access categories (AC) per station, internal collision handling, post-back-off after successful transmission and frame-discarding after maximum retransmission limit. The proposed model has also implemented pre-back-off carrier sensing mechanism and back-off counter freezing with deferred states in both the cases. It has incorporated different carrier sensing and back-off parameters for each active AC for access category wise service differentiation. We have   computed the saturation throughput and frame access delay of each   access category   for both RTS/CTS and basic modes. Analytical model is validated by simulation.

Keywords: *Access Category (AC), Arbitration Inter-Frame Space (AIFS), Enhanced Distributed Channel Access (EDCA), Quality of Service (QoS), Short Interframe Space (SIFS).*

1. Introduction

The enhanced distributed channel access (EDCA) protocol of the emerging IEEE 802.11e standard [1]   supports access category wise quality of service (QoS)   differentiation between the real-time and the non real-time applications. In the last few years, performance analysis of EDCA has attracted the attention of several researchers.

1.1 Related work

The contemporary research articles [2]-[10] on EDCA are all based on simulations. The analytical models [11]-[21] of EDCA have considered only one priority class active AC or flow per station. But the IEEE 802.11e EDCA standard has suggested four simultaneously active access categories (ACs) per station with internal collision handling feature. Also, the models [11], [13]-[14], [16]-[18], [20]-[21]   have not implemented the back-off counter freezing i.e. not decrementing the back-off counter during the channel sensing of pre-transmission back-off process, if the channel goes busy due to the transmissions of other access categories. The model [14] has not considered frame discarding after successful transmission, which reduces excessive frame access delay.

The model proposed by Tao and Panwar [22], Tantra et al. [23], Foh et al. [24] and Hwang et al. [25] have implemented only two priority class ACs per station. These models [23]-[25] have not considered back-off counter freezing for the higher priority class AC. Also, during the freezing process,   the model [22] for the higher priority class AC and the models [22]-[25] for the   lower priority class AC, have not incorporated the appropriate deferred states during the busy channel. Also, no deferred states are implemented during physical carrier sensing, which follows the back-off process.

None of the models [11]-[25] have implemented pre-back-off carrier sensing for any access category with the deferred states. The model proposed by   Kong et al. [26] has also implemented only for two ACs per station. For the purpose of pre-back-off carrier sensing and   channel sensing during the pre-transmission back-off process, it has considered the absolute busy probability of the channel, not the probability of sensing the channel busy by the target   access category. Also, for the pre-back-off carrier sensing and back-off counter freezing, the model   has considered arbitrary values for AIFS and total deferred time for all ACs.

Also, the models [11]–[26] have not   incorporated the standard post back-off after successful transmission which reduces the starvation of lower ACs.

1.2 Scope of our proposed model

The aforesaid models are less accurate and inefficient due to their inability to capture the real situations. The differences between the above models and the model implemented by us are listed as follows:

(i) We have incorporated multiple number of simultaneously active ACs per station which is theoretically unlimited in our solution framework. **(ii)** We have implemented the internal collision handling   feature with the extensive   study of its effect on the performance of EDCA**. (iii)** We have incorporated pre-back-off carrier sensing for continuous *AIFS[i]* duration with deferred states   for   the i_{th} access category AC_i. **(iv)** We have implemented the channel sensing and back-off counter freezing with deferred states   during pre-transmission back-off process, followed by carrier sensing similar to case (iii). **(v)** We have considered the   probability of sensing the channel busy ($p_{i,sb}$ as per equation 14) by the access category AC_i , for both the carrier sensing and back-off counter freezing as mentioned in (iii) and (iv), instead of considering the absolute busy probability of the channel. Also, for both the above cases, we have   considered the exact $AIFS_i$ value of each AC_i, as specified by the IEEE 802.11e standard, instead of choosing   an arbitrary value. Again for both cases, we have computed the exact value of the total deferred time T_i of the target AC_i in the   deferred states, as per computation in equation (20), instead of a choosing an arbitrary value. This computation involves T_i as a function of the successful transmission probabilities of other ACs ($p_{j,su}$) and the collision probability (P_{cl}) which are the equation variables. **(vi)** We have incorporated   the standard post back-off after successful transmission to reduce the starvation of lower ACs. **(vii)** Frame discarding after retry limit which reduces excess frame access delay, is also considered by us.

The implementation of the above mentioned features in our model has made it very accurate, fair and efficient by taking care of the real situations.

The rest of this paper is organized as follows. The proposed analytical model, performance analysis and validation of model are discussed in section 2, 3 and 4 respectively. Finally the conclusion is drawn in section 5.

2. Proposed analytical model

In this section, we have formulated the discrete-time, four dimensional   Markov chain (Fig 1a and Fig 1b) for   our proposed model for the i_{th} ($0 \leq i \leq ac_m - 1$) access category AC_i within a station. Here ac_m is the maximum number of simultaneously active ACs   per station which is theoretically unlimited in our solution framework.   We have assumed ideal channel condition with saturation traffic for each access category. The access category AC_i has its own arbitration inter-frame space number $AIFSN_i$ to compute its $AIFS_i$ (or *AIFS [i]*) value as: $AIFS_i = AIFSN_i * \delta$ +*SIFS*, where δ is the slot time. It has also minimum contention window $W_{i,0}$, maximum contention window $W_{i,m}$ and retry limit parameter $r_{i,m}$.

2.1 Markov *chain formulation*

In our model, time is considered to be slotted. For the access category AC_i at slot time *t*, let *s(i,t), b(i,t)* and *d´(i,t)* be the stochastic processes respectively to denote   back-off stage value   *r*, the back-off counter value *k*, and the *AIFS* counter or deferred states counter value *d*. For the purpose of random back-off, the value of *k* is uniformly drawn from [0 , $W_{i,r} - 1$] where $W_{i,r} = (2)^r W_{i,0}$ and $W_{i,0} \leq W_{i,r} \leq W_{i,m} = 2^{r_{i,m}} W_{i,0}$. Here $W_{i,0}$, $W_{i,r}$ and $W_{i,m}$ are respectively the contention window at back-off stage *0, r* and $r_{i,m}$.

We assume that the conditional collision probability $p_{i,cl}$ of access category AC_i is constant and independent of the   back-off stage *r*. Accordingly, the four - dimensional process *{i, s(i, t), b(i, t),* d *(i, t)}* becomes a discrete-time four-dimensional Markov chain for the access category AC_i. At slot time t, the state of AC_i can be fully described by (i,r,k,d). For the countdown states of *AIFS* counter and that of deferred states counter during the pre-back-off carrier sensing: ($r = c, k = 0$ and $0 \leq d \leq AIFS[i] + T_i$); for pre-transmission back-off process states: $\left(0 \leq r \leq r_{i,m}, \ 0 \leq k \leq W_{i,r} - 1 \text{ and } d = 0\right)$; for the countdown states of the deferred state counter and that of *AIFS* counter during the back-off counter freezing of the pre-transmission back-off process: $\left(0 \leq r \leq r_{i,m}, 1 \leq k \leq W_{i,r} - 1 \text{ and } 1 \leq d \leq AIFS[i] + T_i\right)$; for post-back-off stage: ($r = p, 0 \leq k \leq W - 1$ and $d = 0$).

2.2 The state transition probabilities

Before transmitting a frame, the i_{th} access category AC_i first performs the pre-back-off carrier sensing process to sense the channel continuously free for $AIFS_i$ or *AIFS[i]* period with the following state transitions from (1) to (3) with the non-null transition probabilities:

1) The AC_i first goes from the $AIFS_i$ counter's countdown states ($i,c,0,AIFS_i$) to (i,c,0,0) by decrementing the $AIFS_i$ counter by 1 in each slot time by sensing the channel free with probability $p_{i,sf}$

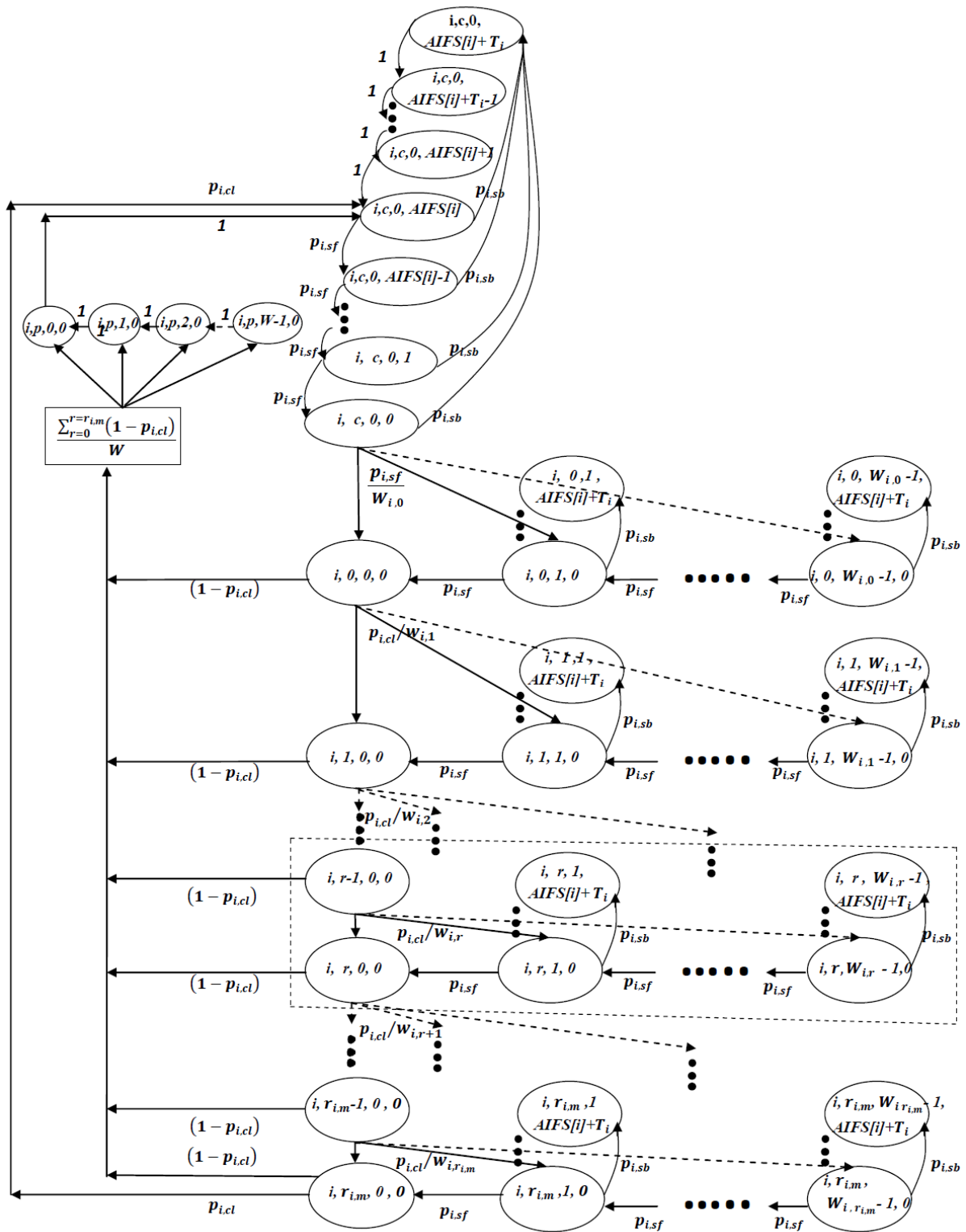$P\{(i, c, 0, d - 1)|(i, c, 0, d)\} = p_{i,sf},$ $1 \leq d \leq AIFS[i]$.

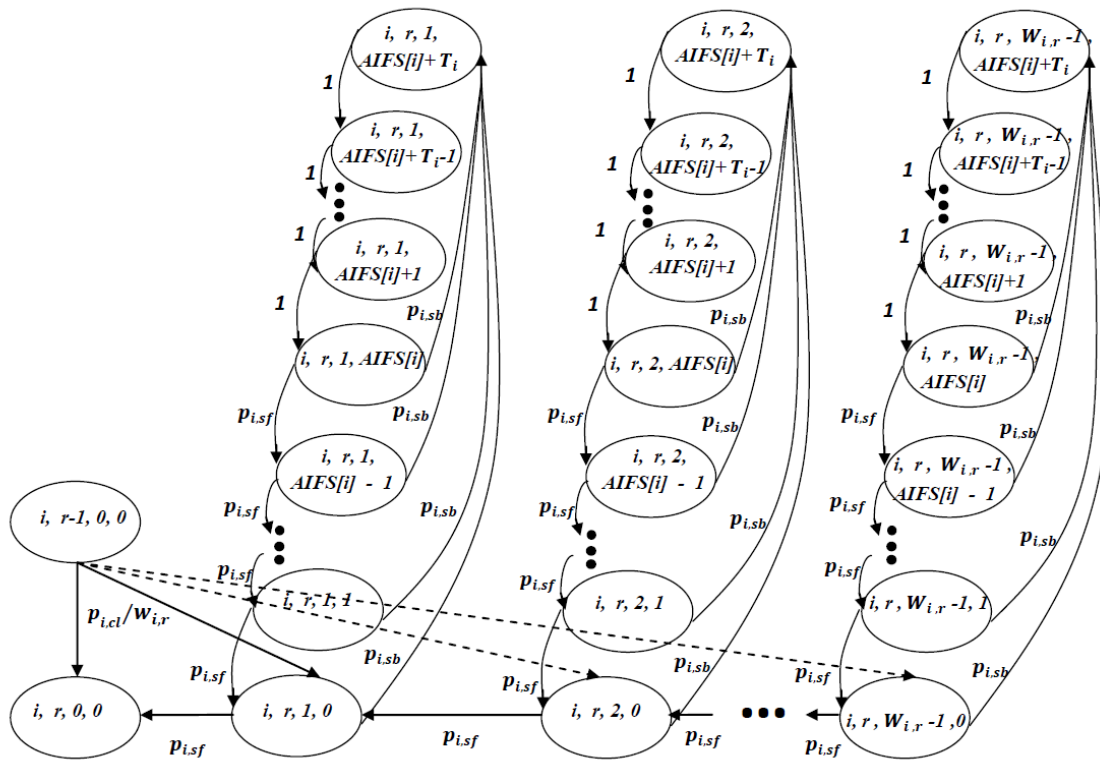Fig 1(a):   Four-dimensional Markov chain for the i_{th} AC.

Fig 1(b): Expanded view of the Markov chain for r_{th} back-off stage of figure (1a).

2) During each of the $AIFS_i$ countdown states of (1) , if the channel goes busy due to the   transmission of other ACs, the AC_i goes to the maximum deferred state $(i, c, 0, AIFS[i] + T_i)$, by sensing the channel busy with the probability $p_{i,sb}$

$$P\{(i,c,0,AIFS[i] + T_i) \mid (i,c,0,d)\} = p_{i,sb}, \quad 0 \le d \le AIFS[i].$$

Where the meaning and the computation process of T_i is explained in equation (20).

3) From the maximum deferred state $(i,\ c,\ 0, AIFS[i] + T_i)$, there is countdown of the deferred state counter by 1 at each slot time

$$P\{(i,c,0,d-1) \mid (i,c,0,d)\} = 1, \quad AIFS[i] + 1 \le d \le AIFS[i] + T_i.$$

Through this countdown process, access category AC_i ultimately goes to the $AIFS_i$ countdown state $(i,c,0,AIFS_i)$ like (1) and recursively follow the state transition procedures (1), (2), and (3), to eventually reach $(i,c,0,0)$ state, to complete pre-back-off carrier sensing process.

4) From the $AIFS_i$ counter's countdown state $(i,c,0,0)$, the pre-transmission back-off process is started for the back-off stage 0, if the channel is free

$$P\{(i,0,k,0) \mid (i,c,0,0)\} = \frac{p_{i,sf}}{W_{i,0}}, \qquad 0 \le k \le W_{i,0} - 1.$$

5) During pre-transmission back-off process of any back-off stage r, the back-off counter is frozen *i.e.* not decremented and the access category AC_i goes to the maximum deferred state $(i,r,k,AIFS[i] + T_i)$, if channel goes busy

$$P\{(i,r,k,AIFS[i] + T_i) \mid (i,r,k,0)\} = p_{i,sb}, \qquad 0 \le r \le r_{i,m} \text{ and } 1 \le k \le W_{i,r} - 1.$$

6) During the frozen period, there is countdown of deferred state counter by 1 at each slot time

$$P\{(i,r,k,d-1)|(i,r,k,d)\} = 1,\ \ 0 \le r \le r_{i,m},\ \ 1 \le k \le W_{i,r} - 1\ and$$

$$AIFS[i] + 1 \le d \le AIFS[i] + T_i.$$

7) After the frozen period elapses by T_i, for the remaining frozen time, the *AIFS[i]* counter is decreased by one, if the channel is free

$$P\{(i,r,k,d-1)|(i,r,k,d)\} = p_{i,sf},\ \ 0 \le r \le r_{i,m}, 1 \le k \le W_{i,r} - 1\ and$$

$$1 \le d \le AIFS[i].$$

Through this transition, AC_i resumes the pre-transmission back-off state $(i,r,k,0)$ after the frozen period.

8) But during the $AIFS[i]$ counter countdown of step 7, if the channel goes busy again due to transmissions of other ACs , AC_i again and goes to the maximum deferred state $(i,r,k,AIFS[i] + T_i)$ like that of step 5.

$$P\{(i,r,k,AIFS[i] + T_i)|(i,r,k,d)\} = p_{i,sb},\ \ 0 \le r \le r_{i,m},\ 1 \le k \le W_{i,r} - 1\ and$$
$$1 \le d \le AIFS[i].$$

Through these transition states (5) to (8), the access category AC_i completes the back-off counter freezing process through transition step 7 and comes back to the pre-transmission back-off process to resume countdown of back-off counter.

9) During pre-transmission back-off process, the back-off counter is decremented by 1, at each slot time, if channel is free, otherwise follow step 5

$$P\{(i,r,k-1,0)|(i,r,k,0)\} = p_{i,sf},\ \ 0 \le r \le r_{i,m}\ and\ 1 \le k \le W_{i,r} - 1.$$

When the back-off counter reaches zero, the access category AC_i transmits the frame.

10) In case of successful transmission, state transition takes place to post-transmission back-off stage *p*, for a random wait interval. This interval is drawn uniformly from the range 0 to *W-1* time slots, where, *W* denotes the post-transmission back-off window, which is same for all ACs

$$P\{(i,p,k,0)|(i,r,0,0)\} = \frac{(1-p_{i,cl})}{W},\ \ 0 \le r \le r_{i,m}\ and\ 0 \le k \le W - 1.$$

11) In case of collision, except during maximum back-off stage $r_{i,m}$, transition takes place to next stage, by doubling the contention window

$$P\{(i,r+1,k,0)|(i,r,0,0)\} = \frac{p_{i,cl}}{W_{i,r+1}},\ \ 0 \le r \le r_{i,m} - 1,\ 0 \le k \le W_{i,r+1} - 1.$$

12) In case of collision at maximum back-off stage $r_{i,m}$, the frame is discarded and transition takes place to the state $(i,c,0,AIFS[i])$ to start the pre-back-off carrier sensing for transmitting a new frame

$$P\{(i,c,0,AIFS[i])|(i,r_{i,m}0,0)\} = p_{i,cl}.$$

13) During post-back-off stage *p*, as there is no channel sensing , the back-off counter is always decremented by one

$$P\{(i,p,k-1,0)|(i,p,k,0)\} = 1,\ 1 \le k \le W - 1.$$

14) After post-transmission back-off process, transition takes place to the state $(i,c,0,AIFS[i])$ to start pre-back-off carrier sensing for transmitting a new frame

$$P\{(i,c,0,AIFS[i])|(i,p,0,0)\} = 1 \ .$$

For state transition for post-transmission back-off stage *p*, as mentioned in the state transition step 10, we have chosen the same post-transmission back-off window *W* for all ACs to satisfy the inequality: $W_{3,0} < W_{2,0} < W < W_{1,0} < W_{0,0}$ with the pre-transmission back-off windows variables $W_{3,0}, W_{2,0}, W_{1,0}, W_{0,0}$. Due to this carefully chosen inequality, the post-transmission back-off process reduces the starvation of the lower ACs *i.e.* AC_0 and AC_1 , by decreasing their post-transmission back-off delay compared to that of the pre-transmission back-off process. Also, unlike pre-transmission back-off process, the transitional probability of decrementing the back-off counter during the post-transmission back-off process is considered one, since the channel sensing is not implemented during this stage. Because, post-transmission back-off is not really meant for the frame transmission like the pre-transmission back-off process. It is performed only for adding some random wait to the recently successfully transmitting access categories to defer their next transmission.

2.3 System equations

Let $b_{i,r,k,d} = lim_{t\to\infty} P\{i, s(i,t) = r, b(i,t) = k, \mathrm{d}(i,t) = d\}$ be the stationary distribution of the four-dimensional Markov chain for the i_{th} AC, for $0 \le i \le ac_m - 1$, $0 \le r \le r_{i,m}$, $0 \le k \le W_{i,r} - 1$ and $0 \le d \le AIFS[i] + T_i$. In steady state, we can derive the following equations through chain regularities

$$b_{i,r,0,0} = b_{i,r-1,0,0}\, p_{i.cl} \to b_{i,r,0,0} = (p_{i.cl})^r\, b_{i,0,0,0}, \qquad 0 \le r \le r_{i,m}. \tag{1}$$

Now using the standard steady state formulation of Markov chain, *w. r. t.* Fig 1(b), for pre-transmission back-off process, we get

$$b_{i,r,k,0} = b_{i,r-1,0,0}\frac{p_{i,cl}}{W_{i,r}} + b_{i,r,k,1}\,p_{i,sf} + b_{i,r,k+1,0}p_{i,sf}, \quad 0 \le r \le r_{i,m}, \ 1 \le k \le W_{i,r} - 1.$$

$$= \frac{b_{i,r,0,0}}{W_{i,r}} + b_{i,r,k,1}\,p_{i,sf} + b_{i,r,k+1,0}p_{i,sf}. \quad \text{(Using the first part of Eq. (1))} \tag{2a}$$

Using chain regularities *w. r. t*. Fig 1(b), we can derive

$$b_{i,r,k,1}\,p_{i,sf} = p_{i,sb}\,b_{i,r,k,0} \to b_{i,r,k,1}\,p_{i,sf} = (1 - p_{i,sf})b_{i,r,k,0} \ . \tag{2b}$$

Putting (2b) in (2a) and interchanging sides we get

$$b_{i,r,k,0} = \frac{b_{i,r,0,0}}{W_{i,r}p_{i,sf}} + b_{i,r,k+1,0} \tag{2c}$$

From (2c), using the regularities of chain we get

$$b_{i,r,k+1,0} = \frac{b_{i,r,0,0}}{W_{i,r}p_{i,sf}} + b_{i,r,k+2,0} \tag{2d}$$

Similarly,

$$b_{i,r,\,W_{i,r}-2,0} = \frac{b_{i,r,0,0}}{W_{i,r}p_{i,sf}} + b_{i,r,\,W_{i,r}-1,0} \tag{2e}$$

Since, for r_{th} stage, $b_{i,r,\,W_{i,r}-1,0}$ is the last element of the chain and there is no state on its right side, we get

$$b_{i,r,\,W_{i,r}-1,0} = \frac{b_{i,r,0,0}}{W_{i,r}\,p_{i,sf}} \tag{2f}$$

Putting (2d) to (2f) in (2c), we get

$$b_{i,r,k,0} = \frac{b_{i,r,0,0}}{W_{i,r}\, p_{i,sf}} + \frac{b_{i,r,0,0}}{W_{i,r}\, p_{i,sf}} + \cdots \frac{b_{i,r,0,0}}{W_{i,r}\, p_{i,sf}} + \frac{b_{i,r,0,0}}{W_{i,r}\, p_{i,sf}}, \; (W_{i,r}-1)-(k-1) = W_{i,r}-k \text{ terms})$$

$$= \frac{W_{i,r}-k}{W_{i,r}} \frac{b_{i,r,0,0}}{p_{i,sf}}.$$

$$= \frac{W_{i,r}-k}{W_{i,r}} \frac{b_{i,r,0,0}}{(1-p_{i,sb})}, \quad 0 \le r \le r_{i,m}, 1 \le k \le W_{i,r}-1, \; d = 0. \tag{2g}$$

For carrier sensing during back-off counter freezing of pre-transmission back-off process, from Eq. (2b), we get

$$b_{i,r,k,1}\, p_{i,sf} = \left(1 - p_{i,sf}\right) b_{i,r,k,0}$$

$$\rightarrow b_{i,r,k,1} = \frac{(1-p_{i,sf})\, b_{i,r,k,0}}{p_{i,sf}}, \quad 0 \le r \le r_{i,m}, 1 \le k \le W_{i,r}-1. \tag{3a}$$

Now using chain relation, w.r.t. Fig 1 (b) we get

$$b_{i,r,k,1} = b_{i,r,k,2}\, p_{i,sf}. \tag{3b}$$

$$\rightarrow b_{i,r,k,2} = \frac{b_{i,r,k,1}}{p_{i,sf}} = \frac{(1-p_{i,sf})\, b_{i,r,k,0}}{p_{i,sf}{}^2}, \quad \text{(Using Eq. (3a) and (3b)).} \tag{3c}$$

Similarly,

$$b_{i,r,k,3} = \frac{b_{i,r,k,2}}{p_{i,sf}} = \frac{(1-p_{i,sf})\, b_{i,r,k,0}}{p_{i,sf}{}^3}. \tag{3d}$$

Through the same reasoning, we get

$$b_{i,r,k,AIFS[i]} = \frac{(1-p_{i,sf})\, b_{i,r,k,0}}{p_{i,sf}{}^{AIFS[i]}}. \tag{3e}$$

Therefore,

$$b_{i,r,k,d} = \frac{(1-p_{i,sf})\, b_{i,r,k,0}}{p_{i,sf}{}^{d}}, 0 \le r \le r_{i,m}, 1 \le k \le W_{i,r}-1 \text{ and } \le d \le AIFS[i]. \tag{3f}$$

For other deferred states during back-off counter freezing, using the chain relationship of Fig 1(b), we get

$$b_{i,r,k,d} = \frac{(1-p_{i,sf})}{(p_{i,sf})^{AIFS[i]}} b_{i,r,k,0},$$

$$0 \le r \le r_{i,m}, 1 \le k \le W_{i,r}-1, AIFS[i]+1 \le d \le AIFS[i]+T_i. \tag{4}$$

Using the chain regularity in the similar way for pre-back-off carrier sensing with the deferred states, we get

$$b_{i,c,0,d} = \frac{1}{(p_{i,sf})^{d+1}} b_{0,0,0,0}, \; 0 \le d \le AIFS[i]. \tag{5}$$

$$b_{i,c,0d} = \frac{1-p_{i,sf}{}^{AIFS[i]+1}}{(p_{i,sf})^{AIFS[i]+1}} b_{0,0,0,0}, \quad AIFS[i]+1 \le d \le AIFS[i]+T_i. \tag{6}$$

For post-back-off stage p, *w.r.t* Fig 1(a),

$$b_{i,p,k,0} = \frac{W-k}{W} b_{i,p,0,0}, \; 0 \le k \le W-1. \tag{7}$$

(Putting $r = p, W_{i,r} = W$ and $p_{i,sb} = 0$ in Eq. (2g), since for post-back-off stage p, back-off counter is decremented with probability of 1)

Also for post-back-off stage p, we can derive

$$b_{i,p,0,0} = \sum_{r=0}^{r_{i,m}} (1 - p_{i,cl})\, b_{i,r,0,0}. \tag{8}$$

Now, since the sum total of the steady state probabilities of all the states of the Markov chain is 1, therefore

$$\sum_{d=0}^{AIFS[i]+T_i} b_{i,c,0,d} + \sum_{r=0}^{r_{i,m}} \sum_{k=0}^{W_{i,r}-1} b_{i,r,k,0} + \sum_{r=0}^{r_{i,m}} \sum_{k=1}^{W_{i,r}-1} \sum_{d=1}^{AIFS[i]+T_i} b_{i,r,k,d} + \sum_{k=0}^{W-1} b_{i,p,k,0} = 1. \quad (9)$$

Using Eq. (1) to Eq. (9) and by simplifying we get

$$b_{i,0,0,0} =$$

$$\left[\left[\left[\frac{\left(1 - p_{i,sf}^{AIFS[i]+1}\right)}{\left(p_{i,sf}\right)^{AIFS[i]+1}} \right] \left[\frac{1 + (1 - p_{i,sf})T_i}{(1 - p_{i,sf})} \right] \right] + \left[\sum_{r=0}^{r_{i,m}} \left[1 + \frac{1}{p_{i,sf}} \frac{(W_{i,r}-1)}{2} \right] (p_{i,cl})^r \right] + \right.$$

$$\left. \left[\sum_{r=0}^{r_{i,m}} \left[\frac{\left(1 - (p_{i,sf})^{AIFS[i]} + (1 - p_{i,sf})T_i\right)}{\left(p_{i,sf}\right)^{AIFS[i]+1}} \frac{(W_{i,r}-1)}{2} \right] (p_{i,cl})^r + \left[(1 - p_{i,cl}) \frac{W+1}{2} \sum_{r=0}^{r_{i,max}} (p_{i,cl})^r \right] \right]^{-1}. \quad (10)$$

Let τ_i be the probability that an AC_i within a station transmits in the channel in a randomly chosen slot time. Since, a transmission occurs in state $(i,r,0,0)$ for all transmission stages $r \in [0,r_{i,m}]$, τ_i may be expressed as the sum of steady state probabilities of all the corresponding $(i,r,0,0)$ states. Therefore

$$\tau_i = \sum_{r=0}^{r_{i,m}} b_{i,r,0,0} = \sum_{r=0}^{r_{i,m}} b_{i,0,0,0} (p_{i,cl})^r = \frac{\left(1 - (p_{i,cl})^{(r_{i,m}+1)}\right)}{(1 - p_{i,cl})} b_{i,0,0,0}, \ 0 \leq i \leq ac_m - 1. \quad (11)$$

Also, let τ be the probability that a station transmits in the channel in a randomly chosen slot time. A station transmits, when at least one of the ACs within that station transmits. Therefore

$$\tau = 1 - \prod_{i=0}^{ac_m-1}(1 - \tau_i). \quad (12)$$

Let $p_{i,sf}$ be the probability that an access category AC_i within a station senses the channel free during pre-back-off carrier sensing and pre-transmission back-off process. The AC_i may sense the channel free, if none of the ACs from the set of remaining ACs within the same station and none from the remaining $(N-1)$ stations transmits. Here N is the total number of stations in the WLAN. Therefore

$$p_{i,sf} = (1 - \tau)^{N-1} \prod_{i' \neq i}(1 - \tau_{i'}), \ 0 \leq i \leq ac_m - 1. \quad (13)$$

Therefore, the probability $p_{i,sb}$, that an access category AC_i within a station senses the channel free, be given as

$$p_{i,sb} = 1 - p_{i,sf}, \ (\text{Since } p_{i,sb} + p_{i,sf} = 1). \quad (14)$$

Let $p_{i,cl}$ be the conditional collision probability *i.e.* the probability that an access category AC_i within a station, while transmitting, sees collision in the channel. Considering both internal and external collisions, such collision would occur when at least one access category from the set of higher ACs within the same station or from the remaining $N-1$ station transmits. Therefore,

$$p_{i,cl} = 1 - (1 - \tau)^{N-1} \prod_{i' > i}(1 - \tau_{i'}). \quad (15)$$

Now, considering all the N stations in the WLAN, let $p_{i,su}$ be the successful transmission probability of an AC_i in the wireless channel. $p_{i,su}$ can be calculated as N times the joint probabilities the following three statistically independent events:

(i) The AC_i within the station is transmitting with probability τ_i,

(ii)   None of the higher ACs than the access category AC_i in the same station is transmitting with   probability $\prod_{i'>i}(1 - \tau_{i'})$,

(iii) None of the remaining (*N-1*) stations are transmitting with probability of

$$(1 - \tau)^{N-1}.$$

Therefore,

$$p_{i,su} = N\tau_i(1 - \tau)^{N-1}\prod_{i'>i}(1 - \tau_{i'}). \tag{16}$$

Now, including all ACs, the total successful transmission probability P_{su} in the channel, is the sum total of the successful transmission probabilities of the individual ACs. Therefore,

$$P_{su} = \sum_{i=0}^{ac_m-1} p_{i,su}. \tag{17}$$

The probability P_{fr}, that the channel is free or idle, is the probability that none of the N stations In the WLAN is transmitting. Therefore

$$P_{fr} = (1 - \tau)^N. \tag{18}$$

Finally, the probability P_{cl}, that collision is taking in the channel is given by

$$P_{cl} = 1 - P_{su} - P_{fr}. \tag{19}$$

Since, the sum total of the probabilities of all the above three events are 1.

Let T_i (in slot time) be the total deferred time of the target access category AC_i. T_i is actually the transmission time of other ACs in slot time that makes the channel busy for the target access category AC_i during the   pre-back-off carrier sensing and back-off counter freezing. T_i is computed as the statistical average   of the expected value of the successful transmission time and collision time of other ACs, divided by the slot time δ and rounded off to the nearest integer. Therefore

$$T_i = \frac{1}{\delta} \frac{\sum_{j=0,j\neq i}^{ac_m-1}(p_{j,su}\,T_{j,su})+P_{cl}T_{cl}}{\sum_{j=0,j\neq i}^{ac_m-1}(p_{j,su})+P_{cl}} \tag{20}$$

Now equations (10) to (20), for $0 \leq i \leq (ac_m - 1)$, give rise to a   total of $(7*ac_m+4)$ non-linear equations with equal number of unknown variables, depending on the   value   of ac_m.   These   variables   are   given   by   the   set: $\{b_{i,0,0,0}, \tau_i, p_{i,sf}, p_{i,sb}, p_{i,cl}, p_{i,su}, T_i \mid (0 \leq i \leq ac_m - 1)\}$ and τ, P_{su}, P_{fr}, and P_{cl}. Here, $T_{i,su}$, T_{cl}, W, $W_{i,0}$, $W_{i,r}$, $r_{i,m}$ are known constants for $0 \leq r \leq r_{i,m}$, $0 \leq i \leq ac_m - 1$ and ac_m is numbers of simultaneously active ACs per stations which is theoretically unlimited in our model. By numerical methods, we have solved the above equations for variables: $\{\tau_i \mid (0 \leq i \leq ac_m - 1)\}$ and τ for any value of ac_m in the same solution framework. Knowing the values of the above variables, subsequent computations are carried out.

3. Performance analysis.

3.1 Saturation throughput computation

The normalized   saturation throughput of AC_i i.e. $Throughput_i$ is defined as the ratio of the expected value of the successful transmission time of the payload *i.e.* $\left(p_{i,su}\,\dfrac{E(P)}{speed_m}\right)$ to the expected value of the total time of transmission .The latter includes:

(i) the average idle time (P_{fr}, δ), (ii) average total successful frame transmission time $\sum_{i=0}^{ac_m-1}(p_{i,su} T_{i,su})$ of all ACs inclusive of payload with headers and (iii) the average time lost in collision $(P_{cl}T_{cl})$ in the channel. Therefore,

$$Throughput_i = \frac{p_{i,su}\frac{E(P)}{speed_m}}{P_{fr}\,\delta + \sum_{i=0}^{ac_m-1}(p_{i,su} T_{i,su}) + P_{cl}\,T_{cl}} \quad . \tag{21}$$

Here $E(P)$ is the expected value of the payload in bits that is transmitted at the MAC speed $(speed_m)$. Also, δ is the slot-time, $T_{i,su}$ is the average successful transmission time of a frame of an access category AC_i and T_{cl} is the average collision time of a frame as formulated in the subsequent equations.
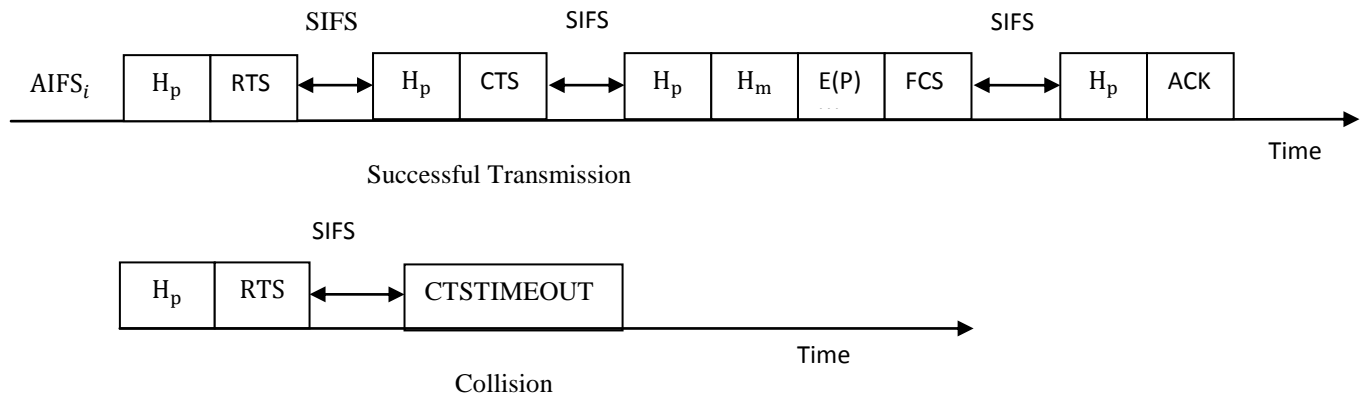

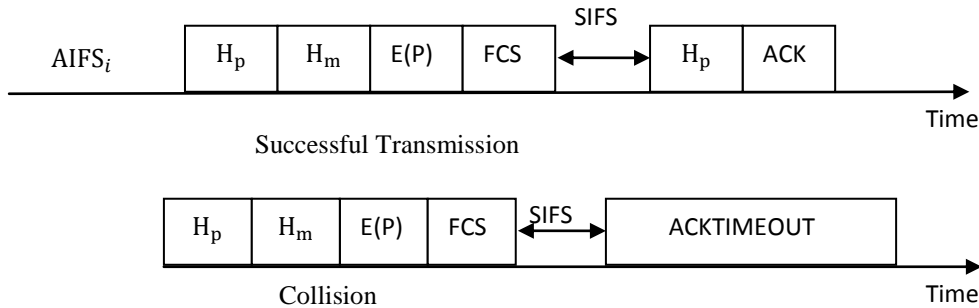Fig 2 (a): Timing Sequence for Transmission of RTS/CTS Mode of Standard EDCA for i_{th} AC.

Fig 2 (b): Timing Sequence for Transmission of Basic Mode of Standard EDCA for i_{th} AC.

Now, $T^{rts}_{i,su}$ and T^{rts}_{cl} (used in Eq. 21 as $T_{i,su}$, T_{cl}) are formulated for RTS/CTS mode , according to Fig 2 (a)

$$T^{rts}_{i,su} = AIFS[i] + \left(\frac{H_p}{speed_p} + \frac{RTS}{speed_m}\right) + \left(\frac{H_p}{speed_p} + \frac{CTS}{speed_m}\right) + \left(\frac{H_p}{speed_p} + \frac{H_m+E(P)+FCS}{speed_m}\right)$$
$$+ \left(\frac{H_p}{speed_p} + \frac{ACK}{speed_m}\right) + 3\,SIFS. \tag{22}$$

Also,

$$T^{rts}_{cl} = \left(\frac{H_p}{speed_p} + \frac{RTS}{speed_m}\right) + SIFS + CTSTIMEOUT. \tag{23}$$

Similarly for the basic access mode, according to Fig 2(b)

$$T^{bas}_{i,su} = AIFS[i] + \left(\frac{H_p}{speed_p} + \frac{H_m+E(P)+FCS}{speed_m}\right) + SIFS + \left(\frac{H_p}{speed_p} + \frac{ACK}{speed_m}\right). \tag{24}$$

Also,

$$T^{bas}{}_{cl} = \left(\frac{H_p}{speed_p} + \frac{H_m + E(p) + FCS}{speed_m} \right) + SIFS + ACKTIMEOUT. \tag{25}$$

The notational meaning and the values above of parameters are presented in table1.

Table 1 802.11e PHY/MAC parameters for analysis and simulation

Payload size [$E(P)$]	1024 bytes	MAC speed [$speed_m$]	11 Mbps
Physical Header [H_p]	192 bits	Slot-time [δ]	20 μs
Data Frame MAC header[H_m]+FCS	288 bits	SIFS	10 μs
RTS frame [RTS]	160 bits	DIFS	2* δ + SIFS
CTS frame [CTS]	112 bits	ACKTIMEOUT	DIFS+ACK
ACK frame [ACK]	112 bits	CTSTIMEOUT	DIFS+CTS
Physical/channel speed [$speed_p$]	1 Mbps	AIFS[AC]	SIFS +AIFSN [AC] * δ

3.2 Saturation delay computation

For the computation of saturation delay, we have followed the model [12] with substantial modifications.

Let $P_{i,st}$ be the probability that a frame of access category AC_i, is successfully transmitted. $P_{i,st}$ is calculated by summing up the probabilities of the successful transmission cases from the first attempt of transmission (with $r = 0$) to the retry limit $r_{i,m}$. Now the probability of r_{th} successful transmission case is: $\left(p_{i,cl} \right)^r \left(1 - p_{i,cl} \right)$. Therefore

$$P_{i,st} = \sum_{r=0}^{r_{i,m}} \left(p_{i,cl} \right)^r \left(1 - p_{i,cl} \right) = 1 - (p_{i,cl})^{r_{i,m}+1}. \tag{26}$$

Let $R_{i,bs}$ be a random variables respectively to denote the total number of back-off slots that a frame of AC_i passes through during the pre-transmission back-off process, till it is successfully transmitted through any of the back-off stages $r \in [\ 0, r_{i,m}]$. When a frame has successful transmission through a back-off stage r, it performs back-off in all stages from stage 0 to r. The average number of back-off slots that a frame passes through, during its back-off process at any arbitrary back-off stage u is: $\sum_{n=1}^{W_{i,u}-1} \frac{n}{W_{i,u}}$. Therefore, total number of back-off slots a frame undergoes when it has successful transmission through a back-off stage r is: $\sum_{u=0}^{r} \sum_{n=1}^{W_{i,u}-1} \frac{n}{W_{i,u}}$. Now the conditional probability of successful transmission of a frame through back-off stage r is: $\frac{p_{i,cl}{}^r (1-p_{i,cl})}{P_{i,st}}$. Therefore the expected value of the total number of back-off slots *i.e.* $E(R_{i,bs})$, is given by

$$E(R_{i,bs}) = \sum_{r=0}^{r_{i,m}} \frac{p_{i,cl}{}^r (1-p_{i,cl})}{P_{i,st}} \sum_{u=0}^{r} \sum_{n=1}^{W_{i,u}-1} \frac{n}{W_{i,u}} \tag{27}$$

Let $R_{i,bf}$ be random variables to denote the total instances back-off counter freezing that a frame of access category AC_i passes through during the back-off process, till it is successfully transmitted through any of the back-off stages $r \in [\ 0, r_{i,m}]$. Since the expected

value of total instances back-off counter freezing $i.e.$ $E(R_{i,bf})$ is proportional to $E\left(R_{i,bs}\right)$ and $p_{i,sb}$ as per Eq. (14), hence

$$E\left(R_{i,bf}\right) = E(R_{i,bs})\frac{p_{i,sb}}{p_{i,sb}+p_{i,sb}}. \tag{28}$$

Let $R_{i,rt}$ be a random variable denoting the total number of retransmissions, for a frame of AC_i, before its successful transmission. Hence , through the similar reasoning

$$E\left(R_{i,rt}\right) = \sum_{r=0}^{r_{i,m}} \frac{r\left(p_{i,cl}\right)^r\left(1-p_{i,cl}\right)}{P_{i,st}}. \tag{29}$$

Let $FRAME_{i,delay}$ be a random variable denoting the total saturation frame access delay for a frame of access category AC_i, before its successful transmission. Therefore, for the RTS/CTS and basic mode

$$E\left(FRAME_{i,delay}\right) = E(R_{i,bs})\delta + E(R_{i,bf})T_{i,bf} + E(R_{i,rt})\left(T_{i,cs}+T_{cl}\right) + \left(T_{i,cs}+T_{i,su}\right). \tag{30}$$

Where $T_{i,bf}$ and $T_{i,cs}$ are respectively the   time spent in each instance of back-off counter freezing and carrier sensing for an AC_i. We calculate $T_{i,bf}$ and $T_{i,cs}$ in the following way:

To calculate $T_{i,bf}$, let $Delay\ (i,r,k,\mathrm{d})$ be the delay of the state (i,r,k,d) due to freezing $w.\ r.\ t$ the state $(i,r,k,0)$. Following the chain relationship of the Markov chain for the back-off counter freezing, for $0 \le r \le r_{i,m}$, $1 \le k \le W_{i,r}-1$, we get

$$Delay\left(i,r,k,d\right) = Delay\left(i,r,k,d-1\right)+\delta,\ \ AIFS[i]+1 \le d \le AIFS[i]+T_i. \tag{31}$$

For the remaining frozen states

$$Delay\left(i,r,k,d\right) = p_{i,sb}\ Delay\left(i,r,k,AIFS[i]+T_i\right) + p_{i,sf}\ Delay\left(i,r,k,d-1\right)+\delta,$$

$$1 \le d \le AIFS[i]. \tag{32}$$

Therefore,

$$T_{i,bf} = Delay\left(i,r,k,AIFS[i]+T_i\right) - Delay(i,r,k,0). \tag{33}$$

Since all the delays are calculated $w.\ r.\ t.$ state $(i,r,k,0)$ we can assume

$$Delay(i,r,k,0) = 0. \tag{34}$$

The equation number (31) to (34) gives rise to $AIFS[i]+T_i+2$ number of equations (for $0 \le i \le ac_m-1$)   with equal number of variables, which are solved for $Delay$ (i,r,k,d) for $0 \le d \le AIFS[i]+T_i$ and $T_{i,bf}$.

To calculate $T_{i,cs}$, let $Delay\ (i,c,0,d)$ be the delay of the state $(i,c,0,d)$ due to carrier sensing $w.\ r.\ t$ the state $(i,c,0,0)$.   Following the chain relationship of the Markov chain for the pre-back-off carrier sensing, we get

$$Delay\left(i,c,0,d\right) = Delay\left(i,c,0,d-1\right)+\delta,\ \ AIFS[i]+1 \le d \le AIFS[i]+T_i. \tag{35}$$

Now, for the remaining frozen states

$$Delay\left(i,c,0,d\right)$$
$$= p_{i,sb}\ Delay\left(i,c,0,AIFS[i]+T_i\right)+p_{i,sf}\ Delay(i,c,0,d-1)+\delta\ ,\ \ 1 \le d \le AIFS[i].$$
$$\tag{36}$$

Therefore,

$$T_{i,cs} = Delay\ (i,c,0,AIFS[i]) - Delay\ (i,c,0,0). \tag{37}$$

Since all the delays are calculated *w. r. t.* state $(i,c,0,0)$ we can assume

$$Delay\ (i,c,0,0) = 0. \tag{38}$$

The equation number (35) to (38) give rise to $AIFS[i] + T_i + 2$ number of equations with equal number of variables, which are solved for *Delay $(i,c,0,d)$ for $0 \le d \le AIFS[i] + T_i$* and $T_{i,cs}$.

4. Validation of model

The number of simultaneous active ACs within a station in our model is theoretically unlimited. But for simplicity and without the loss of generality, we have considered 4 ACs *i.e.* AC_0, AC_1, AC_2 and AC_3 to satisfy the requirements of IEEE 802.11e EDCA standard. Here, AC_0 is the lowest and AC_3 is the highest priority access category. For service differentiation, each access category AC_i $(0 \le i \le 3)$ has its own parameter values like Arbitration Inter-Frame Space Number $AIFSN_i$, Minimum Contention Window $W_{i,0}$, Maximum Contention Window $W_{i,m}$ and retry Limit $r_{i,m}$. This is presented in the following sets: AIFSN set $= \{AIFSN_0, AIFSN_1, AIFSN_2, AIFSN_3\}$; W_0 set $= \{W_{0,0}, W_{1,0}, W_{2,0}, W_{3,0}\}$, W_m set $= \{W_{0,m}, W_{1,m}, W_{2,m}, W_{3,m}\}$ and R_m set $= \{r_{0,m}, r_{1,m}, r_{2,m}, r_{3,m}\}$. We have incorporated the following inequalities for service differentiation between ACs: $W_{0,0} > W_{1,0} > W_{2,0} > W_{3,0}$; $AIFSN_0 > AIFSN_1 > AIFSN_2 > AIFSN_3$ .We have investigated the performance features of EDCA with the variations of $AIFSN_i$ and $W_{i,0}$ parameters for each AC_i $(0 \le i \le 3)$. we have also studied the effect of internal collision handling on the performance of EDCA.

4.1 Comparison of simulation and analytical results

The simulation of the proposed model has been carried out in NS2 [27] network simulator. NS2 is the most popular network simulator among the researchers because of its open source code and continuous development process. We have extended NS2 by adding additional code in C++ and linking it to the existing code. For simulation purpose, we have considered 4 ACs per station. We have used constant bit rate traffic with its rate higher than the link capacity to implement the saturation traffic condition. Also, each AC within a station transmits fixed size UDP packets. For performance measurement, we have repeated simulations 25 times for each case. The final results of simulations are obtained by taking their average. All the parameters used for numerical computations and simulation purpose are listed in table 1. The physical header is transmitted at 1 mbps, physical /channel bit rate. The AC transmits the MAC header, payload and FCS at 11 mbps (MAC) bit rate.

Comparisons of analytical values TPT-AC0, TPT-AC1, TPT-AC2, TPT-AC3 to simulation values TPT-AC0-simu, TPT-AC1-simu, TPT-AC2-simu and TPT-AC3-simu of table 2 for throughput and analytical values DLY-AC0, DLY-AC1, DLY-AC2 DLY-AC3 to simulation values DLY-AC0-simu, DLY-AC1-simu, DLY-AC2-simu, DLY-AC3-simu of table 3 for delay, show that the simulation results of throughput and delay matches well to the corresponding analytical values.

Table 2 Comparisons of analytical saturation throughput values with simulation results for RTS-CTS mode. W_0 set = {32, 16, 8, 4}, R_m set = {8, 8, 8, 8}, *AIFSN* set {7,5,3,2}.

Number of stations ↓	RTS/CTS THROUGHPUT (ANALYTICAL)			
	TPT-AC0	TPT-AC1	TPT--AC2	TPT--AC3
10	0.0240232	0.0493119	0.104185	0.571863
30	0.0283589	0.0573533	0.117334	0.524607
50	0.0291765	0.058777	0.119286	0.511991
70	0.0294487	0.0592186	0.119745	0.505019
Number of stations ↓	RTS/CTS THROUGHPUT (SIMULATION)			
	TPT- AC0-simu	TPT-AC1-simu	TPT- AC2-simu	TPT-AC3-simu
10	0.0234226	0.04849	0.103143	0.568499
30	0.026232	0.0544856	0.113814	0.515349
50	0.0255294	0.0538789	0.113322	0.496932
70	0.0242952	0.0523098	0.111363	0.484224

Table 3 Comparisons of analytical saturation delay values with simulation results for RTS-CTS mode. W_0 set = {32, 16, 8, 4}, R_m set = {8, 8, 8, 8}, *AIFSN* set {7, 5, 3, 2}.

Number of stations ↓	RTS/CTS DELAY (seconds) (ANALYTICAL)			
	DLY-AC0	DLY-AC1	DLY-AC2	DLY-AC3
10	0.0988839	0.0487648	0.0235815	0.00503722
30	0.165004	0.0821613	0.0406335	0.00980654
50	0.206411	0.103008	0.0512031	0.012618
70	0.235792	0.11778	0.0586725	0.0145771
Number of stations ↓	RTS/CTS DELAY (seconds) (SIMULATION)			
	DLY-AC0--simu	DLY-AC1-simu	DLY--AC2-simu	DLY-AC3-simu
10	0.0984344	0.048521	0.0234131	0.00497425
30	0.162754	0.0809289	0.0397628	0.00943879
50	0.20172	0.100433	0.0493744	0.0118294
70	0.22829	0.113658	0.0557389	0.0133016

4.2 Service differentiation

For both RTS/CTS and basic mode with any W_0, R_m and *AIFSN* set, for any number of stations, the throughput and delay maintains the following inequalities: $\text{Throughput}_{AC3} > \text{Throughput}_{AC2} > \text{Throughput}_{AC1} > \text{Throughput}_{AC0}$ (table 4) and $\text{Delay}_{AC3} < \text{Delay}_{AC2} < \text{Delay}_{AC1} < \text{Delay}_{AC0}$ (table 5). This service differentiation is because of the following in-built inequalities of the model: $W_{0,0} > W_{1,0} > W_{2,0} > W_{3,0}$; $AIFSN_0 > AIFSN_1 > AIFSN_2 > AIFSN_3$ and also due to the implementation of the internal collision handler.

Table 4 Saturation throughput comparisons between RTS/CTS and basic mode. W_0 set = {32, 16, 8, 4}, R_m set ={8, 8, 8, 8}, AIFSN set {7, 5, 3, 2}.

Number of stations ↓	RTS/CTS THROUGHPUT			
	AC0	AC1	AC2	AC3
10	0.0240232	0.0493119	0.104185	0.571863
30	0.0283589	0.0573533	0.117334	0.524607
50	0.0291765	0.058777	0.119286	0.511991
70	0.0294487	0.0592186	0.119745	0.505019
Number of stations ↓	Basic THROUGHPUT			
	AC0	AC1	AC2	AC3
10	0.017025	0.0349469	0.0738349	0.405274
30	0.0177637	0.0359255	0.0734971	0.328609
50	0.0170543	0.0343563	0.0697254	0.299269
70	0.0163553	0.032889	0.0665043	0.280479

Table 5 Saturation delay comparisons between RTS/CTS and Basic mode. W_0 set = {32, 16, 8, 4}, R_m set = {8, 8, 8, 8}, AIFSN set {7, 5, 3, 2}.

Number of stations ↓	RTS/CTS DELAY (seconds)			
	AC0	AC1	AC2	AC3
10	0.0988839	0.0487648	0.0235815	0.00503722
30	0.165004	0.0821613	0.0406335	0.00980654
50	0.206411	0.103008	0.0512031	0.012618
70	0.235792	0.11778	0.0586725	0.0145771
Number of stations ↓	BASIC DELAY (seconds)			
	AC0	AC1	AC2	AC3
10	0.138553	0.068657	0.0335616	0.00759115
30	0.260258	0.129999	0.0647526	0.016226
50	0.347891	0.174057	0.0870305	0.0221187
70	0.417338	0.20893	0.104619	0.0267048

4.3 RTS/CTS and basic mode comparison

With the same W_0 set = {32,16,8,2}, R_m set ={8,8,8,8} and $AIFSN$ set = {7,5,3,2}, it is observed that, for any number of stations, for any AC_i, the normalized saturation throughput for RTS/CTS mode is always higher than that of the basic mode as shown in table 4 and the saturation delay for RTS/CTS mode measured in seconds is always lower than that of the basic mode as shown in table 5, because of lesser collision loss of RTS/CTS mode.
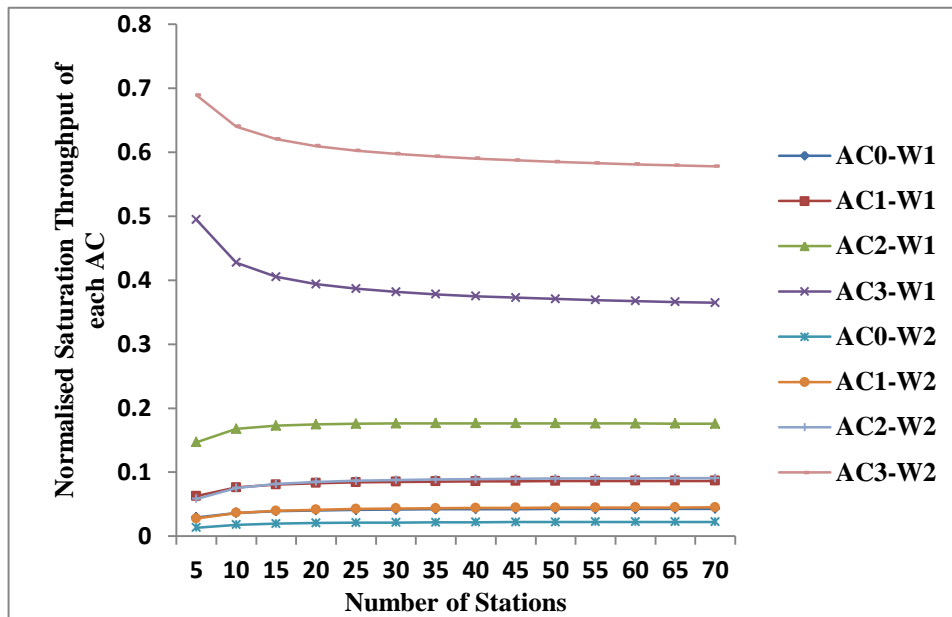
Fig 3: RTS/CTS Throughput with the Variation of Contention Window. For Case W1: W_o Set ={16,8,4,2}, for Case W2: W_o Set ={48,24,12,2}. For Both the Cases, *AIFSN* set = {7,5,3,2}, R_m set {8,8,8,8}.
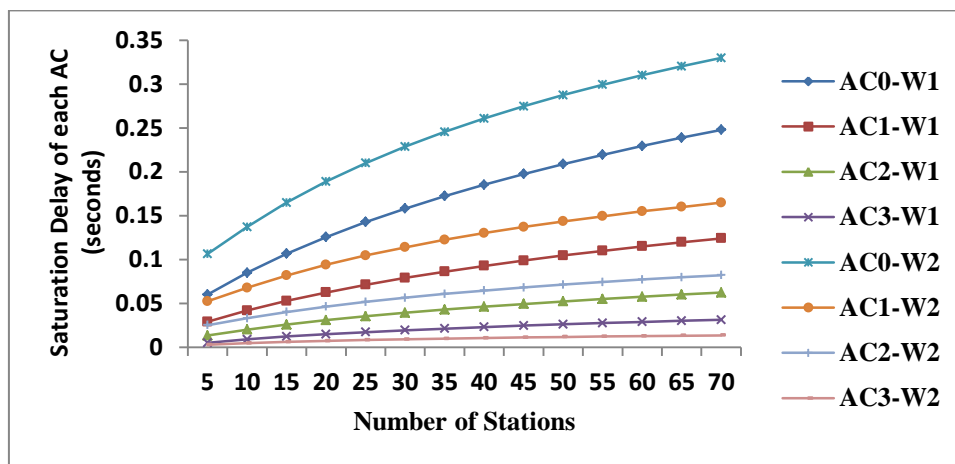

Fig 4: RTS/CTS Delay with the Variation of Contention Window. For Case W1: W_o Set ={16,8,4,2}, for Case W2: W_o Set ={48,24,12,2}. For Both the Cases, *AIFSN* Set = {7,5,3,2}, R_m Set {8,8,8,8}.

4.4 Effect of Contention Window variation

To show the effect of contention window variation on saturation throughput (Fig 3) and saturation delay (Fig 4) of RTS/CTS mode, we have considered two different cases of contention windows *i.e.* W1 and W2. For case W1: W_0 set = {16,8,4,2} and for case W2: W_0 set = {48,24,12,2}. In both the cases the contention window of access category AC_3 is kept at the same low value of 2, whereas in case W2 , the contention window values of AC_2, AC_1 and AC_0 are kept at higher values. Because of this, access category AC_3 gets more chances of winning the channel in case W2, due to its comparatively lesser waiting time in pre-transmission back-off process. Therefore, the throughput of AC_3 in case W2 (Fig 3) increases and the delay of access category AC_3 in case of W2 (Fig 4) decreases. The throughput and delay of access categories AC_2, AC_1, AC_0 in case of W2   follows the reverse trend.

4.5 Effect of Contention Window variation on total throughput

From table 6, it is observed that as the contention window set W_0 is moved from = {16,8,4,2} to {64, 32, 16, 2}, the total saturation throughput keeps on increasing. This is because, in the latter contention window sets, the spread of the contention window values from lower to higher ACs increases. Therefore, the total collision probability in the channel decreases and the total throughput increases.

Table 6 Total throughput with contention window W_0 set variation for RTS/CTS mode.

R_m set = {8, 8, 8, 8}, AIFSN set {7, 5,3, 2}.

RTS/CTS TOTAL THROUGHPUT				
W_0 set →	{16,8,4,2}	{32,16,8,2}	{48,24,12,2}	{64,32,16,2}
Number of Stations ↓	THROUGHPUT TOTAL	THROUGHPUT TOTAL	THROUGHPUT TOTAL	THROUGHPUT TOTAL
10	0.707458	0.749383	0.76946	0.781151
30	0.684174	0.727653	0.749653	0.762909
50	0.675478	0.71923	0.741562	0.755112
70	0.669513	0.713431	0.735897	0.749562

4.6 Effect of AIFSN variation

To show the effect of AIFSN variation on saturation throughput (Fig 5) and saturation delay (Fig 6) of RTS/CTS mode, we have considered two different cases of *AIFSN i.e.* A1 and A2. For case A1: *AIFSN* set = {7,5,3,2} and for case A2: *AIFSN* set = {10,7,5,2}. In both the cases, the *AIFSN* values of access category AC_3 is kept at the same low value of 2 , whereas, in case A2, the *AIFSN* values of access categories AC_2, AC_1 and AC_0 are kept at higher values. Because of this, access category AC_3 get more chances of winning the channel in case W2, due to its comparatively much lesser waiting time in pre-back-off carrier sensing process. Therefore, the throughput of AC_3 in case of A2 (Fig 5) increases and the delay of the AC_3 of case of A2 (Fig 6) decreases. The throughput and delay of access categories AC_2, AC_1 and AC_0 of case A2 follows the reverse pattern.
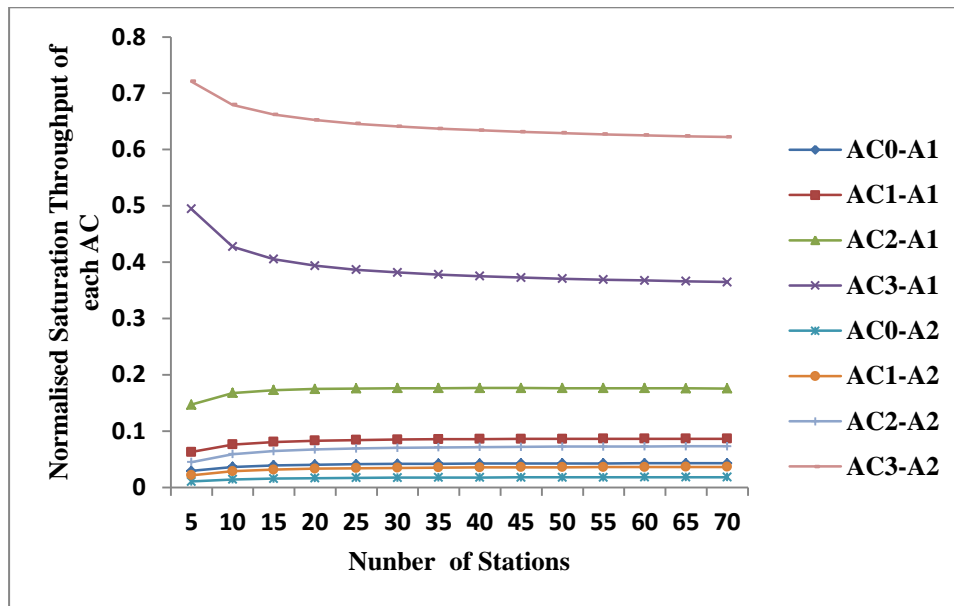
Fig. 5 RTS/CTS Throughput with the Variation of AIFSN Value. For Case A1, $AIFSN$ Set ={7,5,3,2}, for Case A2, $AIFSN$ Set ={10,7,5,2}. For Both the Cases, W_0 set = {16,8,4,2}, R_m set {8,8,8,8}.
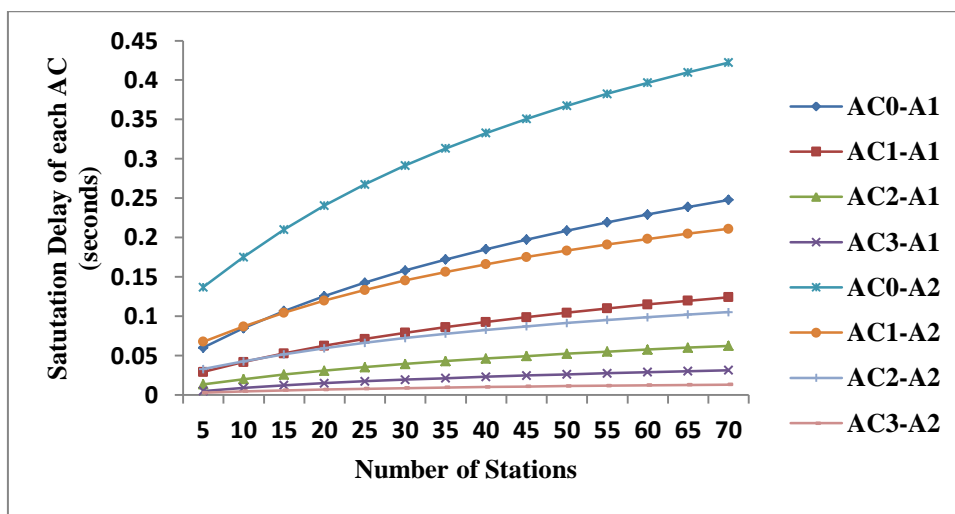

Fig. 6 RTS/CTS delay with the Variation of AIFSN Value. For Case A1, $AIFSN$ set ={7,5,3,2}, for Case A2, AIFSN Set ={10,7,5,2}. For Both the Cases, W_0 Set = {16,8,4,2}, R_m set {8,8,8,8}.

4.7 Effect of Internal collision handler

To compare the performance results without and with internal collision handler of RTS/CTS mode for normalized saturation throughput and saturation delay we have considered same W_0 set ={5,4,3,2}, R_m set = {8,8,8,8} and $AIFSN$ set = {7,5,3,2} in both cases. From the table 7 and table 8 for saturation throughput and table 9 and table 10 for saturation delay, the following observations are made:

(a) For throughput, there is highest   increase for AC_3 and highest decrease for AC_0 with internal collision handler compared to that without the internal collision handler. This is expected due to highest favor of internal collision handler to highest Access

Category. The throughput of intermediate ACs *i.e.* AC_2 and AC_1 are also decreased with AC_1 having higher decrease due to the same reason. Also, due to the same reason, the saturation delay pattern follows the reverse trend.

(b) The effect of internal collision is most dominant at the lower number of stations as expected and it fades away at the higher number of stations due to more external collisions.

Table 7 Saturation throughput of RTS/CTS mode without and with internal collision handler. W_0 set = {5,4,3,2}, R_m set = {8, 8, 8, 8}, AIFSN set {7,5,3, 2}.

Number of stations ↓	RTS/CTS THROUGHPUT WITHOUT INTERNAL COLLISION HANDLER			
	AC0	AC1	AC2	AC3
2	0.0737118	0.102251	0.163358	0.502274
6	0.109387	0.143742	0.207718	0.366243
10	0.115587	0.149355	0.209753	0.346597
18	0.119345	0.152294	0.209594	0.332617
34	0.120934	0.152997	0.207811	0.322005
50	0.120805	0.152267	0.205701	0.315543
Number of stations ↓	RTS/CTS THROUGHPUT WITH INTERNAL COLLISION HANDLER			
	AC0	AC1	AC2	AC3
2	0.0407684	0.0590968	0.101747	0.640672
6	0.092312	0.127169	0.197716	0.409232
10	0.105184	0.140241	0.206051	0.369185
18	0.113822	0.147815	0.208352	0.343362
34	0.118301	0.150961	0.207391	0.326747
50	0.119319	0.151144	0.20549	0.318108

Table 8 Saturation throughput increase (%) of RTS/CTS mode with internal collision handler, compared to that without internal collision handler. W_0 set = {5,4,3,2}, R_m set = {8, 8, 8, 8}, AIFSN set {7,5,3, 2}.

Number of stations ↓	RTS/CTS % THROUGHPUT INCREASE WITH INTERNAL COLLISION HANDLER			
	AC0	AC1	AC2	AC3
2	-44.6922	-42.2042	-37.7153	27.5543
6	-15.6097	-11.5297	-4.81518	11.7378
10	-9.00015	-6.10224	-1.76493	6.51708
18	-4.62776	-2.94102	-0.592574	3.23044
34	-2.17722	-1.33075	-0.202107	1.47265
50	-1.23008	-0.73752	-0.102576	0.812884

Table 9 Saturation delay of RTS/CTS mode without and with internal collision handler. W_0 set = {5,4,3,2}, R_m set = {8, 8, 8, 8}, AIFSN set {7,5,3, 2}.

Number of stations ↓	RTS/CTS DELAY (seconds) WITHOUT INTERNAL COLLISION HANDLER			
	AC0	AC1	AC2	AC3
2	0.0107001	0.00840443	0.00603405	0.00229723
6	0.0167376	0.0135739	0.0103751	0.00563709
10	0.0217559	0.0178126	0.0138268	0.00771689
18	0.0292141	0.0240947	0.0189036	0.0106049
34	0.0392364	0.0325491	0.0257279	0.0142011
50	0.0475868	0.0396345	0.0314736	0.0169068
Number of stations ↓	RTS/CTS DELAY (seconds) WITH INTERNAL COLLISION HANDLER			
	AC0	AC1	AC2	AC3
2	0.0163569	0.0123673	0.00860359	0.00160043
6	0.0190883	0.0148763	0.0108773	0.00440085
10	0.0237173	0.0189065	0.014294	0.0064547
18	0.0309604	0.0251402	0.0194933	0.00941265
34	0.0406779	0.0334252	0.0263165	0.0132702
50	0.04838	0.0399533	0.0316516	0.0163956

Table 10 Saturation delay increase (%) of RTS/CTS mode with internal collision handler, compared to that without internal collision handler. W_0 set = {5,4,3,2}, R_m set = {8, 8, 8, 8}, AIFSN set {7,5,3, 2}.

Number of stations ↓	RTS/CTS % DELAY INCREASE WITH INTERNAL COLLISION HANDLER			
	AC0	AC1	AC2	AC3
2	52.8668	47.1522	42.584	-30.3322
6	14.0444	9.59488	4.84044	-21.9305
10	9.01549	6.14116	3.37895	-16.3562
18	5.97759	4.33913	3.11951	-11.2424
34	3.67388	2.69163	2.28779	-6.55513
50	1.66685	0.80435	0.565553	-3.02364

5. Conclusion

In the analytical model of this research article, we have studied the performance features of EDCA mode of operation of WLAN based on IEEE 802.11e standard . From the analytical and simulation results discussed in section 4, we draw the following conclusions:

1. Analytical and simulation results match well for both normalized saturation throughput and saturation delay and validate our model.

2. The throughput and delay pattern of standard EDCA shows the access category wise QoS differentiation feature, with higher ACs having higher throughput and lower delay. This shows that EDCA is suitable for soft real-time application, when the latter is being run through higher ACs.

3. RTS/CTS mode is better than the basic mode for both throughput and delay because of less collision loss.

4. Contention window and *AIFSN* variation is very effective means of service differentiation between the ACs.

5. Internal collision handler has dominating effect on system performance enhancement for higher ACs at lower load.

In this research article, our key research contributions are:

(i) Implementation of pre-back-off carrier sensing with actual deferred states.

(ii) Implementation of back-off counter freezing during the channel sensing of pre-transmission back-off process with actual deferred   states followed by carrier sensing with deferred states.

(iii) The contemporary EDCA models have implemented only one or at best two priority class active ACs per station whereas we have incorporated multiple number of simultaneously active ACs within each station (theoretically unlimited) denoted by ac_m, in the same solution framework.

(iv) To implement ac_m (theoretically unlimited) number of ACs per station, we have solved a total of ($7*ac_m+4$) numbers of non-linear equations, depending on the value of ac_m, in the same solution framework.

(v) We have elaborately demonstrated the effect of internal collision handler on the performance of EDCA and established the fact that at low load, the internal collision handler plays a very crucial role in the performance enhancement of EDCA, making it more suitable for real-time applications.

(vi) We have implemented frame discarding after retry limit which reduces excessive frame access delay.

(vii) We have also implemented post-back-off after successful transmission to add fairness to the EDCA mode of operation.

References

[1]   Wireless LAN Medium Access Control (MAC) and Physical Layer (PHY) Specifications, IEEE Std 802.11™-2007-Revision of IEEE Std 802.11-1999.

[2]   Mangold S, Choi S, May P, Klein O, Hiertz G, and Stibor L, "IEEE 802.11e Wireless LAN for Quality of Service", In Proc. European Wireless, Florence, Italy, Feb.2002, pp. 32-39.

[3]   Choi S, "Emerging IEEE 802.11e WLAN for Quality-of-Service (QoS) provisioning," SK Telecomm. Rev., Vol. 12, no.6, 2002, pp. 894–906.

[4]   Grilo A, and Nunes M, "Performance evaluation of IEEE 802.11e," In Proc. PIMRC, Sep.2002, pp. 511–517.

[5]   Choi S, Prado J D, Shankar S and Mangold S, "IEEE 802.11e contention-based channel access (EDCF) performance evaluation," In Proc. IEEE ICC, vol. 2, May 2003, pp. 1151–1156.

[6]   He D and Shen C Q, "Simulation study of IEEE 802.11e EDCF," In Proc. 57th IEEE Semiannu. VTC, Apr. 2003, pp. 685–689.

[7]   Mangold S, Choi S, Hiertz G R, Klein O and Walke B, "Analysis of IEEE 802.11e for QoS support in wireless LANs," IEEE Wireless Communications, December 2003, pp.40-50.

[8]   Lindgren A, Almquist A, and Schelen O, "Quality of service schemes for IEEE 802.11 wireless LANs—an evaluation," Mobile Networks, Vol. 8, 2003, pp. 223–235.

[9]   Ni Q, "Performance analysis and enhancements for IEEE 802.11e wireless networks" IEEE Network, July/August 2005, pp.21-27.

[10]   Xiao Y, "IEEE 802.11E: QoS provisioning at the MAC layer", IEEE Wireless Communications, June 2004, pp.72-79.

[11]   Robinson J W, Randhawa TS,   "Saturation throughput analysis of IEEE 802.11e enhanced distributed coordination function", IEEE Journal of Selected Areas in Communication, Vol. 22, no. 5, pp. 917–928.

[12]   Xiao Y, "Performance analysis of priority schemes for IEEE 802.11 and IEEE 802.11e wireless LANs", IEEE Transactions in Wireless Communications ,Vol. 4, no. 4, 2005, pp. 1506–1515.

[13]   Zhu H, Chlamtac I, "Performance analysis for IEEE 802.11e EDCF service differentiation", IEEE Transactions on Wireless Communications, Vol.4, no.4, 2005, pp. 1779–1788.

[14]   Hui J and Devetsikiotis M, "A unified model for the performance analysis of IEEE 802.11e EDCA", IEEE Transactions in Communications, Vol.53, no. 9, 2005, pp. 1498–1510.

[15]   Hwang G H, and Cho D H, "Performance analysis on coexistence of EDCA and legacy DCF stations in IEEE 802.11 wireless LANs", IEEE Transactions on Wireless Communications, Vol.5, no.12, 2006, pp.3355-3359.

[16]   Chen X, Zhai H, Tian X, and Fang Y, "Supporting QoS in IEEE 802.11e wireless LANS", IEEE Transactions on Wireless Communications, Vol.5, no. 8, 2006, pp. 2217-2227.

[17]   Tantra J W, Foh C H, Tinnirello I and Bianchi G, "Analysis of the IEEE 802.11e EDCA under statistical traffic," In Proc. IEEE ICC '06, June 2006, pp. 546-551.

[18]   Zhao L, Wu J Y, Zhang H and Zhang, J "Integrated quality-of-service differentiation over IEEE802.11 wireless LANs", IET Communications, Vol.2, no.2, 2008, pp. 329–335.

[19]   Gao D, Cai J, Foh C H , Lau C and Ngan K N, "Improving WLAN VoIP capacity through service differentiation", IEEE Transactions on Vehicular Technology, Vol. 57, no.1, 2008, pp. 465-474.

[20]   Inan I, Keceli F and Ayanoglu E, "Analysis of the 802.11e enhanced distributed channel access function", IEEE Transactions on Communications, Vol. 57, no.6 , 2009, pp. 1753-1764.

[21]   Peng F, Peng B and Qian D, "Performance analysis of IEEE 802.11e enhanced distributed channel access", IET Communications, Vol.4, no.6, 2010, pp. 728–738.

[22]   Tao Z, and Panwar S, "Throughput and delay analysis for the IEEE 802.11e enhanced distributed channel access", IEEE Transactions on Communications, Vol.54, no. 4, 2006, pp. 596–603.

[23]   Tantra J W, Foh C H and Mnaouer A B, "Throughput and delay analysis of the IEEE 802.11e EDCA saturation", In Proc. IEEE International Conference on Communications (ICC), May 2005, pp. 3450-3454.

[24]   Foh C H, Zhang Y, Ni Z, Cai J, and Ngan K N, "Optimised cross-layer design for scalable video transmission over the IEEE 802.11e networks", IEEE Transactions   on Circuits and Systems for video Technology,   Vol. X, no. XX XXX, 2007, pp. 1-14.

[25]   Hwang H Y, Kim S J , Sung D K, Song N O, "Performance analysis of IEEE 802.11e EDCA with a virtual collision handler" , IEEE Transactions on Vehicular Technology, Vol. 57, no.2, 2008, pp. 1293-1297.

[26]   Kong Z , Tsang D H K, Bensaou B and Gao D, "Performance analysis of the IEEE 802.11e contention-based channel access," IEEE Journal of Selected Areas in Communications, Vol. 22, no. 10, 2004, pp. 2095–2106.

[27]   The Network Simulator2—NS2: http://www.isi.edu/nsnam/ns.